JACS
JOURNAL OF THE AMERICAN CHEMICAL SOCIETY

Article

Understanding Reactivity and Stereoselectivity in Palladium-Catalyzed Diastereoselective sp3 C–H Bond Activation: Intermediate Characterization and Computational Studies

Ramesh Giri, Peng Liu, Yu Lan, K. N. Houk, and Jin-Quan Yu

J. Am. Chem. Soc., **Just Accepted Manuscript** • DOI: 10.1021/ja304643e • Publication Date (Web): 25 Jul 2012

Journal of the American Chemical Society is published by the American Chemical Society. 1155 Sixteenth Street N.W., Washington, DC 20036

Understanding Reactivity and Stereoselectivity in Palladium-Catalyzed Diastereoselective sp^3 C–H Bond Activation: Intermediate Characterization and Computational Studies

Ramesh Giri,[†] Yu Lan,[‡] Peng Liu,[‡] K. N. Houk[‡] and Jin-Quan Yu*[†]*

[†]Department of Chemistry, The Scripps Research Institute, 10550 North Torrey Pines Road, La Jolla, California 92037 [‡]Department of Chemistry and Biochemistry, University of California, Los Angeles, California 90095.

yu200@scripps.edu; houk@chem.ucla.edu

RECEIVED DATE (to be automatically inserted after your manuscript is accepted if required according to the journal that you are submitting your paper to)

†The Scripps Research Institute

‡University of California

Abstract. The origin of the high levels of reactivity and diastereoselectivity (>99:1 dr) observed in the oxazoline-directed, Pd(II)-catalyzed sp^3 C–H bond iodination and acetoxylation reactions as reported in previous publications has been studied and explained based on experimental and computational investigations. The characterization of a trinuclear chiral C–H insertion intermediate by X-ray paved the way for further investigations into C–H insertion step through the lens of stereochemistry.

Computational investigations on reactivities and diastereoselectivities of C–H activation of *t*-Bu- and *i*-Pr-substituted oxazolines provided good agreement with the experimental results. Theoretical predictions with DFT calculations revealed that the most preferred transition state for C–H activation contains these two sterically bulky *t*-Bu substituents in *anti*-positions due to steric repulsion, and that this transition state leads to the major diastereomer which is consistent with the structure of the newly characterized C–H insertion intermediate. The structural information about the transition state also suggests that a minimum dihedral angle between C–H bonds and Pd–OAc bonds is crucial for C–H bond cleavages. We have also utilized density functional theory (DFT) to calculate the energies of various potential intermediates and transition states with *t*-Bu and *i*-Pr substituted oxazolines, and suggested a possible explanation for the substantial difference in reactivity between the *t*-Bu and *i*-Pr substituted oxazolines.

1. Introduction

Transition metal-catalyzed activation/functionalization of unactivated C–H bonds has been the subject of great research interest in recent years.[1, 2] Among the plethora of transition metal-catalyzed processes, palladium-catalyzed reactions, in particular, have enjoyed a prominent standing in the C–H activation field.[3] In addition to innovation of diverse reactions, detailed mechanistic pathways, particularly concerning the discrete steps involved in the catalytic processes, are being meticulously investigated from both theoretical standpoints[4, 5, 6, 7] and experimental studies.[8, 9] Despite remarkable progress in these two frontiers with palladium catalysts, stereoselective cleavage of unactivated prochiral C–H bonds and its mechanistic aspects have been little explored.[10] The diastereotopic C–H bonds at the carbon atom are selectively cleaved on a metal center under the influence of a proximal chiral center tethered to it *via* a removable linkage.[11] Tolman and coworkers observed a moderate level of diastereoselectivity in the intramolecular activation of sp^3 C–H bonds in a rhodium dicarbonyl complex of C_3-symmetric TpMenth ligand.[12] Although these metal-mediated reactions show stereoselectivity during the C–H activation step, subsequent functionalization of the metallacycles has been realized only

in limited cases. Sames and coworkers have described the total synthesis of (–)-rhazinilam based on the diastereoselective dehydrogenation of an ethyl group *via* C–H activation by attaching a synthetic intermediate to a stoichiometric dialkyl Pt-chiral oxazoline complex through an imine linkage.[13] Tremendous efforts have also been devoted to develop transition metal-catalyzed asymmetric C–H functionalization in the areas of allylic acetoxylation,[14] biomimetic oxidation,[15] addition of arene to alkene[16] and carbenoid/nitrenoid insertion.[2, 17] In this regard, we reported a rare example of auxiliary-controlled asymmetric Pd insertion into both sp^2 and sp^3 C–H bonds. Selection of an appropriate auxiliary or directing group that would effect C–H bond cleavage with palladium catalysts under mild conditions is crucial for high stereoselectivity. While asymmetric induction through installation of chiral auxiliary is a well-established procedure in organic synthesis,[18] extension of this approach to the catalytic, stereoselective activation of C–H bonds is largely unexplored. We were encouraged by Meyer's α-lithiation/alkylation chemistry, where chiral oxazolines provide high levels of asymmetric induction,[19] and the success of using chiral oxazolines as ligands in asymmetric catalysis.[20] Furthermore, previously observed oxazoline-directed cyclopalladation reactions of both sp^2 and sp^3 C–H bonds[21] also provided the foundation for our exploratory studies.

We began our investigation by proposing a working steric model for diastereoselective cleavage of C–H bonds on organic molecules pre-coordinated to a transition metal through a removable, non-racemic, chiral linkage (Scheme 1). Since σ-chelation-assisted C–H activation takes place through a cyclic transition state,[5] we envisioned that the selection of oxazoline as a cyclic chiral auxiliary would provide an efficient stereocontrol by forming a conformationally rigid bicyclic transition state **1** during C–H bond cleavage. As a consequence, the chiral auxiliary could induce high levels of stereoselectivity during C–H activation in conjunction with a bicyclic conformation *via* a steric repulsion model outlined in Scheme 1. Transition state **1a**, in which the sterically bulky R^1 and R^2 groups are in *anti*-position, is favored over **1b** due to reduced steric repulsion between Me and R^2 when R^1 is larger than the Me

group. Predominant C–H activation pathway through transition state **1a** will give the major stereoisomer.

Scheme 1. Working model for diastereoselective C–H cleavage

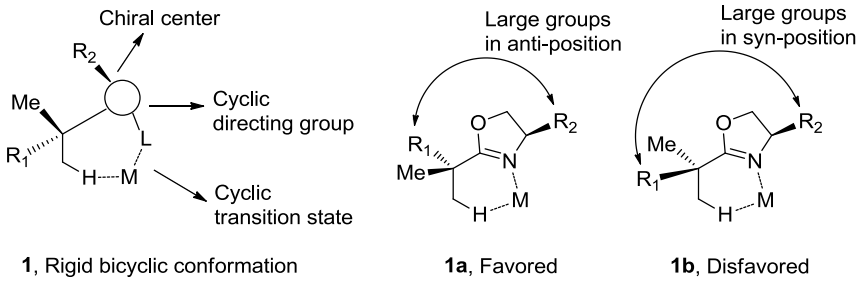

Our early investigations were long baffled by the lack of reactivity and stereoselectivity of oxazolines bearing 4-*i*-Pr group such as **2c** (R^1 = Et, R^2 = *i*-Pr; 15% yield, 0% de) for the iodination of β-C–H bonds (Scheme 2). Strikingly, reactions proceeded with high yields and moderate diastereoselectivity when the 4-*i*-Pr group was replaced by a 4-*t*-Bu group (**2b**, R^1 = Et, R^2 = *t*-Bu; 91% yield, 25% de). Moreover, substitution of Et group at the α-position of the parent carboxylic acid with sterically demanding *t*-Bu group, such as in oxazoline **2a**, afforded *mono*-iodinated product **3a** in 83% yield with a high level of diastereoselectivity (82% de) (Scheme 2).

Intrigued by the dramatic change in reactivity and stereoselectivity with subtle alterations in the steric environment on the oxazoline ring, we have sought, in the present study, to elucidate the mechanism and origin of reactivity and diastereoselectivity through the preparation and characterization of a reactive intermediate formed after diastereoselective C–H activation, and computational studies on the energies of possible intermediates and transition states leading to the isolated intermediate using density functional theory (DFT).[22] Our computational investigation has revealed that the reactions with *i*-Pr and *t*-Bu-substituted oxazolines involve different catalyst resting states before C–H activation, and that the lower reactivity of an *i*-Pr-substituted oxazoline results from greater stability of its catalyst resting state, which accounts for higher overall activation barrier for C–H cleavage. We have also characterized by a single crystal X-ray crystallography the major isomer of a chiral trinuclear palladacycle formed after

diastereoselective cleavage of a β-C–H bond of a chiral oxazoline bearing two diastereotopic methyl groups. In excellent agreement with the solid state structure, theoretical predictions with density functional theory (DFT) calculations also revealed that the most preferred transition state for C–H activation in oxazoline substrates contains sterically bulky substituents at the α-position of parent carboxylic acid and the oxazoline ring in *anti*-positions due to steric repulsion, and that this transition state leads to the major diastereomer.

Scheme 2. Diastereoselective C–H iodination with *i*-Pr and *t*-Bu substituted oxazoline auxiliaries

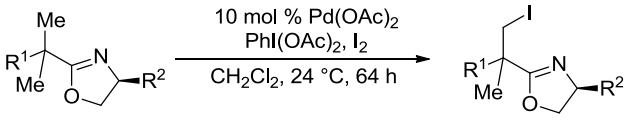

2

2a, $R^1 = R^2 = t$-Bu
2b, R^1 = Et, $R^2 = t$-Bu
2c, R^1 = Et, $R^2 = i$-Pr

3

3a, $R^1 = R^2 = t$-Bu; 83% yield, 82% de
3b, R^1 = Et, $R^2 = t$-Bu; 91% yield, 25% de
3c, R^1 = Et, $R^2 = i$-Pr, 15% yield, 0% de

2. Results and Discussion

We previously prepared the cyclopalladated trinuclear complexes **5**, **6** and **8** of achiral and chiral oxazolines **4** and **7** (Scheme 3).[9, 23] These palladacycles are potential intermediates in the Pd(II)-catalyzed iodination and acetoxylation of unactivated C–H bonds.[9] First, these palladacycles maintain trinuclear integrity in the reaction solvent (CH_2Cl_2). The trinuclear complexes distinguish themselves from dimer and monomer by the ratio of acetate groups to oxazoline units as indicated by ^{1}H NMR. Second, they react with iodine and peroxide/acetic anhydride at room temperature to afford the iodinated and acetoxylated products in high yields. Examination of the X-ray crystal structures of these highly reactive trinuclear Pd(II)-complexes **5** and **8** led us to propose a stereomodel to account for diastereoselectivity.[24] In sharp contrast to the 3:2 mixture of *anti*- and *syn*-complexes **5** and **6** formed from achiral oxazoline **4**, only the *anti*-isomer **8** was obtained from the chiral oxazoline **7**. However, we had not characterized intermediates that contain chiral centers on both auxiliary and substrate, which are crucial for elucidating the stereomodel and transition state.

Scheme 3. Trinuclear Pd(II)-complexes with achiral and chiral oxazolines

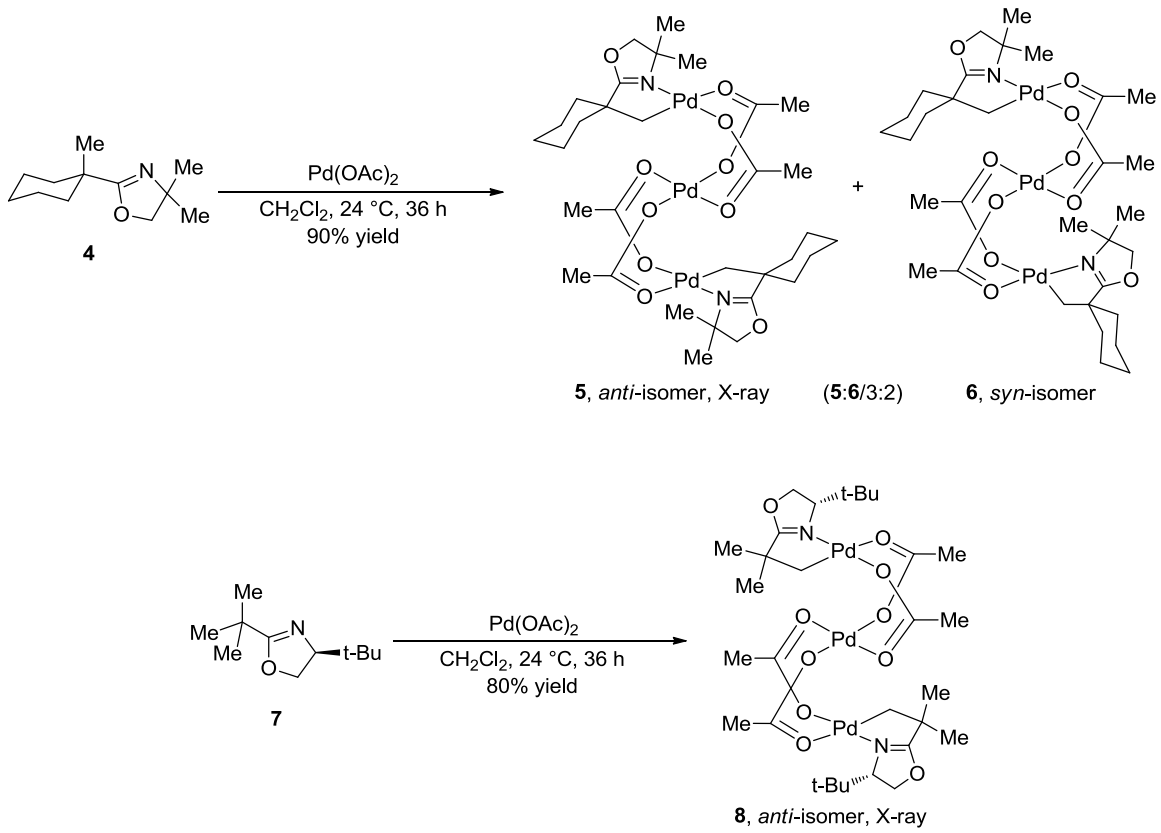

To gain insights into the absolute stereochemistry of the observed C–H activation, we prepared the cyclometallated intermediate **9a** from the reaction of $Pd(OAc)_2$ with the chiral oxazoline **2a** containing diastereotopic methyl groups on the parent carboxylic acid moiety (Scheme 4). The complex **9a** contains a mixture of isomers in a 91:9 ratio, which approximately corresponds to the observed diastereoselectivity. The complex **9a** is highly soluble in *n*-pentane even at −18 ºC, and its purification and crystallization proved extremely difficult. However, we discovered that the bridging μ-acetato groups could be easily exchanged with μ-trifluoroacetato groups without losing the stereoisomeric ratio (91:9) by simply stirring the complex **9a** in trifluoroacetic anhydride for 24 h at room temperature. We were then able to isolate palladacycle **10a** with bridging μ-trifluoroacetato groups and grow a single crystal at −18 °C, which was characterized to be the major isomer ***syn*-(*S*,*S*)-10a** by X-ray crystallography. As predicted, the *t*-Bu groups on the carboxylic acid and oxazoline moieties were oriented in *anti*-positions at both termini of the trinuclear palladacycle ***syn*-(*S*,*S*)-10a**. As a result, the

newly generated chiral center assumed (*S*)-configuration.[25] Moreover, the reaction of μ-acetato palladacycle **9a** with iodine affords the iodinated product in the same diastereoisomeric ratio (91:9).

Scheme 4. Determination of absolute stereochemistry of C–H activation

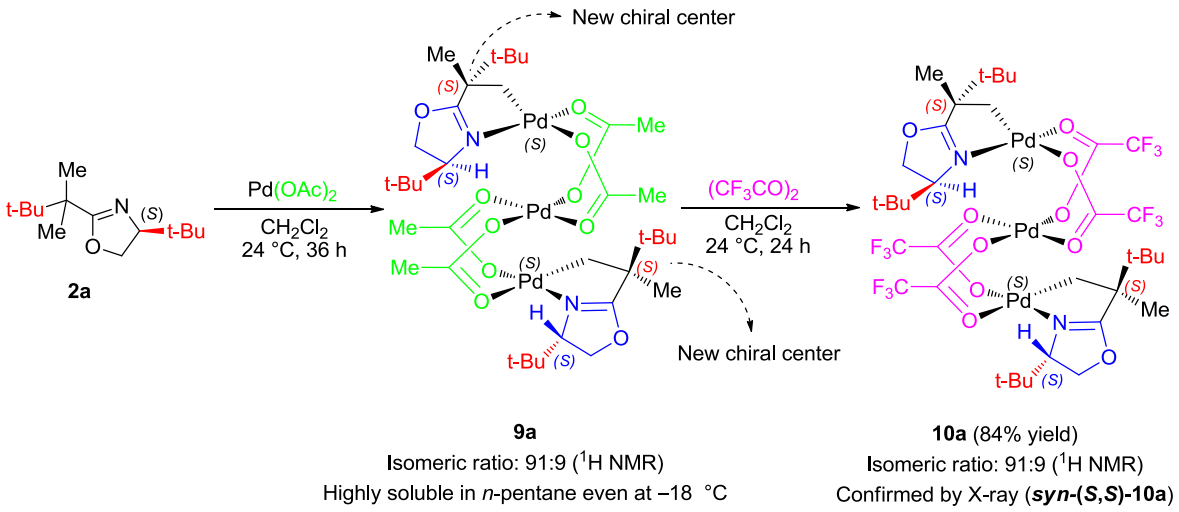

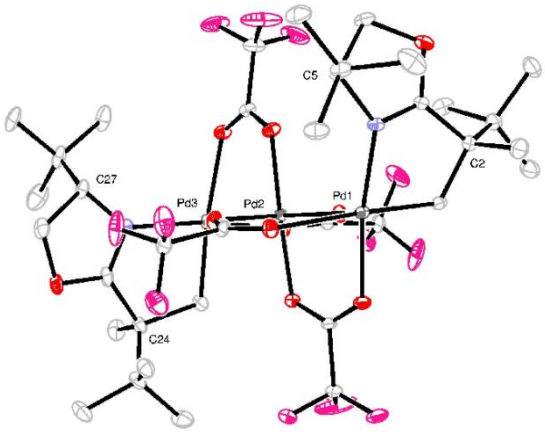

Figure 1. ORTEP diagram of palladacycle ***syn*-(*S*,*S*)-10a**. Selected bond lengths (Å) and angles (deg): C1–Pd1, 1.991(8); C23–Pd3, 1.994(8); N1–Pd1, 2.001(6); N2–Pd3, 2.023(6); Pd1–Pd2, 2.9458(8); Pd2–Pd3, 2.9539(8); C1–Pd1–N1, 81.0(3); C23–Pd3–N2, 83.1(3).

To further investigate the effects of substituents on reactivity and the origin of the high level of diastereoselectivity during the C–H bond cleavage, we performed density functional theory (DFT) studies to calculate the energies of different intermediates and transition states leading to the formation of trinuclear intermediate **9**. Despite extensive computational studies on C–H cleavage involving

ArPdX(PPh_3) species by Maseras and Echavarren,[4] and Fagnou,[6] understanding of cyclopalladation reactions with Pd(II) catalysts remains less developed. In an early mechanistic study of aryl C–H cyclopalladation, Martinez proposed a proton abstraction pathway involving a four-membered transition state.[26] Subsequent computational work by Davies and Macgregor in 2005 supported a similar mechanism, but involving a six-membered transition state.[5] These computational studies indicated that a vacant coordination site on palladium is necessary for insertion into the C–H bond. Based on these previous mechanistic studies, a proposed mechanism of the formation of trinuclear palladacycle **9** is outlined in Scheme 5. The $Pd_3(OAc)_6$ trimer[27] reacts with two molecules of oxazoline **2** to generate intermediate **11**, which dissociates upon further coordination with **2** to form monomeric intermediates **12** or **13** with either one or two oxazolines bound to Pd. The Pd in **12** and **13** adopts a square planar geometry. In intermediate **13**, one of the acetato groups is η-2 coordinated to palladium while the other acetato is η-1 coordinated. The η-2 acetato isomerizes to be η-1 coordinated and releases a vacant coordination site on Pd for subsequent C–H activation. In the C–H activation transition state **14-ts**, the cleavage of C–H bond and formations of the Pd–C and AcO–H bonds are concerted. The structure of **14-ts** suggests that maintaining a minimum dihedral angle between C–H bonds and Pd–OAc bonds are essential for high reactivity. The C–H activation leads to a monomeric palladacycle intermediate **15**. After the release of acetic acid, the trimeric palladacycle complex **9** is generated. Alternatively, the C–H activation may occur with the Pd trimer **11** via transition state **17-ts** instead of its dissociation to monomeric Pd species before C–H activation. This requires breaking one of bridged acetato groups to generate a free coordination site on Pd for C–H activation. Both pathways were considered in the computational investigations.

Scheme 5. The proposed mechanism of the $Pd(OAc)_2$ catalyzed C–H activation of oxazoline **2**.

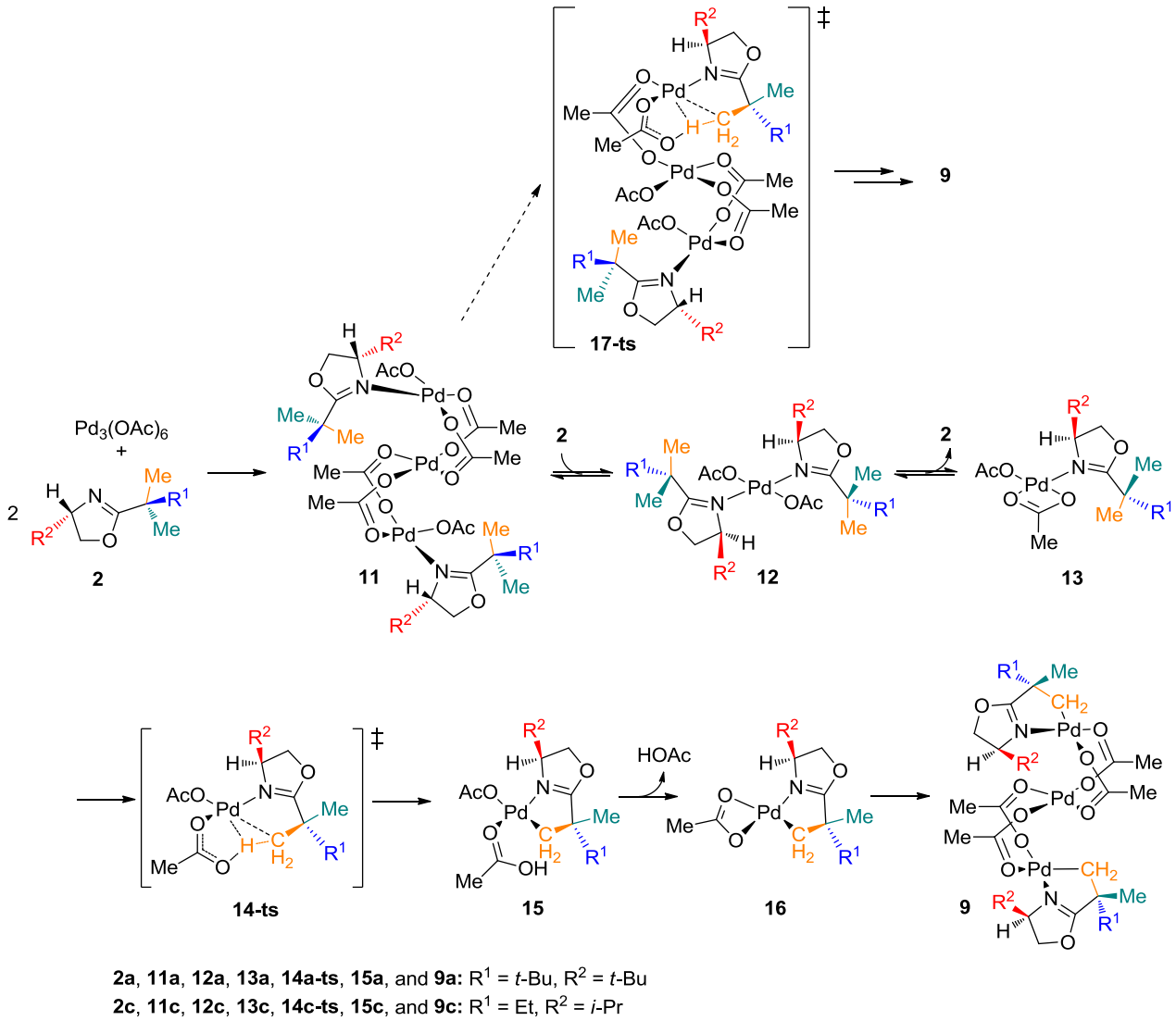

The free energy profiles of C–H activation of oxazolines **2a** (R^1 = *t*-Bu, R^2 = *t*-Bu) and **2c** (R^1 = Et, R^2 = *i*-Pr) are shown in Figure 2. Coordination of two molecules of oxazoline **2c** to the $Pd_3(OAc)_6$ trimer to form complex **11c** is exergonic by 6.8 kcal/mol. The same process with bulkier oxazoline **2a** to form **11a** is endergonic by 9.3 kcal/mol. Further coordination of oxazoline **2c** leads to decomposition of complex **11c** to form monomeric [bis(oxazoline)]$Pd(OAc)_2$ complex **12c**, which is 10.4 kcal/mol more stable than $Pd_3(OAc)_6$. In the reaction with oxazoline **2a**, the Pd monomer complex **12a** is 2.5 kcal/mol less stable than $Pd_3(OAc)_6$. Dissociation of one molecular oxazoline from **12a** and **12c** to form **13a** and **13c** are endergonic by 6.9 and 17.1 kcal/mol, respectively. Thus, in the reaction with the bulkier

oxazoline **2a**, the catalyst resting state before C–H activation is $Pd_3(OAc)_6$, while in the reaction with **2c**, the resting state is the monomeric [bis(oxazoline)]$Pd(OAc)_2$ complex **12c**. The stability of the resting state **12c** leads to significantly higher overall activation energies for C–H activation of oxazoline **2c**. Although the C–H activation transition state **14c-ts** is only 1.8 kcal/mol less stable than the **14a-ts**, the overall activation barrier for reaction with **2c** is 38.4 kcal/mol (**12c** → **14c-ts**), much higher than that for the reaction with **2a** in which the overall barrier is 26.2 kcal/mol ($Pd_3(OAc)_6$ → **14a-ts**). The C–H activation leads to the five-membered metallacycle intermediate, **15a**, and **15c**, respectively. Subsequent elimination of acetic acid from **15a** and **15c** leads to **16a** and **16c**, both are a few kcal/mol less stable than **15a/c** in terms of Gibbs free energies. Association of two molecules of **16a/c** and Pd(OAc)2 forms stable trinuclear Pd metallacycles **9a** and **9c**. Both **9a** and **9c** are ~11 kcal/mol more stable than the monomeric metallacycle **15a** and **15c**. We have also computed single point solvation energy corrections using the SMD model and the results are summarized in the supporting information. In the solvation-corrected free energy diagram, the maximum deviations from the gas-phase results are within a few kcal/mol. The relative activation free energies in gas-phase and in solution only differ by a few tenth of a kcal/mol. These solvation effects do not change any conclusions of the gas phase results.

The alternative pathway which involves C–H activation directly from the trinuclear complexes **11a** and **11c** is less favorable than the mononuclear pathway described above. Trinuclear C–H activation transition states **17a-ts** and **17c-ts** are 7.2 and 3.1 kcal/mol less favorable than the corresponding mononuclear C–H activation transition states (**14a-ts** and **14c-ts**, respectively). The C–H activation from the trinuclear complex requires breaking one of the bridged acetato groups to generate a free coordination site on Pd. This leads to the higher activation energies of the trinuclear pathway.

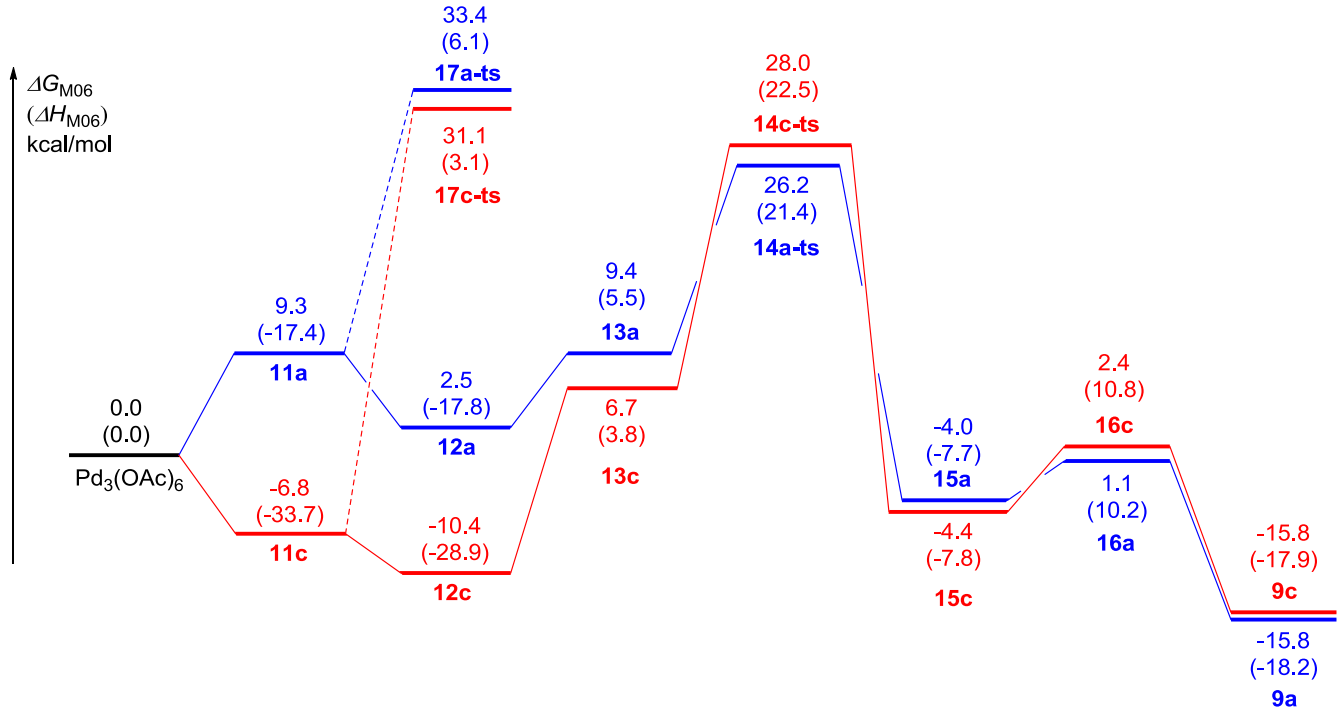

Figure 2. The M06 free energy profile of C–H activation of oxazolines **2a** (blue) and **2c** (red). Enthalpies are given in parentheses.

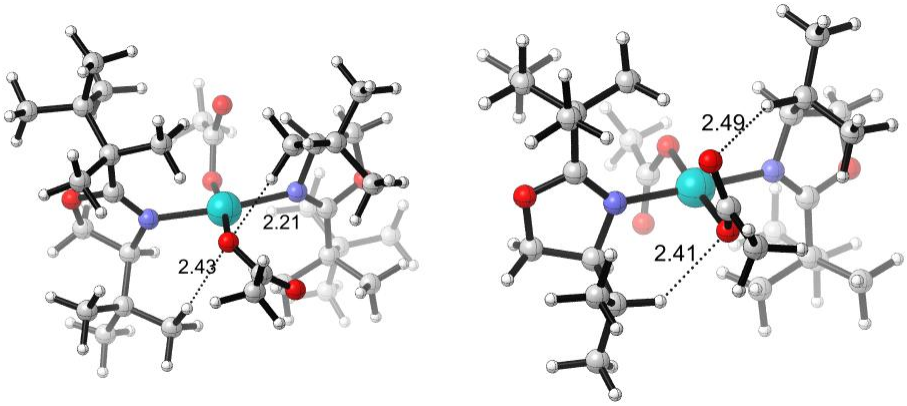

12a (ΔG = 2.5 kcal/mol) **12c** (ΔG = –10.4 kcal/mol)

Figure 3. Optimized geometries of [bis(oxazoline)]Pd(OAc)$_2$ complexes **12a** and **12c**. Energies are with respect to $Pd_3(OAc)_6$.

The optimized geometries of the bis(oxazoline) Pd-complexes **12a** and **12c** are shown in Figure 3. Complex **12a** is destabilized due to steric repulsions of the *t*-Bu (R^2) groups with the acetate. In **12a**, the shortest O–H distances between the *t*-Bu hydrogen and acetate oxygen atoms are 2.21 and 2.43 Å.

Replacing the *t*-Bu group with an *i*-Pr group, the complex **12c** is much less crowded, and thus more stable than **12a**.

We then investigated the origin of stereoselectivity in C–H activations of oxazolines **2a-c**. For each oxazoline, the C–H activation may occur via four possible transition states (**14-ts1** – **14-ts4**, Scheme 6). The optimized geometries of the C–H activation transition states with oxazoline **2a** are shown in Figure 4. All four transition states involve simultaneous cleavage of the C–H bond and formation of the AcO–H and Pd–C bonds as well as strong Pd–H interaction, which indicate a concerted metalation-deprotonation mechanism and a rigid cyclic transition state structure. The six-membered cycle that involves Pd, two atoms in the oxazoline ring, the prochiral α-carbon, and the C–H bond being cleaved, adopts a half-chair conformation. In **14-ts1** and **14-ts3**, the proton being transferred is above the Pd-oxazoline plane, and the α-substituent that is *syn* to R^2 (Me and R^1 in **14-ts1** and **14-ts3**, respectively) is at the axial position. In **14-ts2** and **14-ts4**, the *syn* α-substituent is equatorial (Me and R^1 in **14-ts2** and **14-ts4**, respectively). The R^1 and R^2 groups are *anti* to each other in **14-ts1** and **14-ts2**, which lead to the major diastereomeric (*S*,*S*)-product. R^1 and R^2 are *syn* in **14-ts3** and **14-ts4**, leading to the minor (*S*,*R*)-diastereomer. The computed relative activation energies are summarized in Table 1. In the reactions with **2a** and **2b**, **14-ts1** and **14-ts3** are more than 2 kcal/mol less stable than **14-ts2** and **14-ts4**. Transition states **14-ts1** and **14-ts3** are destabilized by steric repulsions between the axial substituents on the α-carbon and the *t*-Bu (R^2) on the oxazoline. When a smaller R^2 group (*i*-Pr) is employed, **14c-ts1** and **14c-ts3** are only a few tenths kcal/mol less stable than **14c-ts2** and **14c-ts4**. In the reactions with all three oxazolines, the diastereoselectivity of the C–H activation product is determined by the energy difference between **14-ts2** and **14-ts4**. In the reaction with **2a**, **14a-ts2** is 2.3 kcal/mol more stable than **14a-ts4**. This suggests the *syn* product **(*S*,*S*)-15a** is favored with 96% *de*. In the reactions with **2b** and **2c**, the energy difference between **14-ts2** and **14-ts4** is diminished, in agreement with the low *de* observed in experiment.

Scheme 6. Possible transition states of the C–H activation.

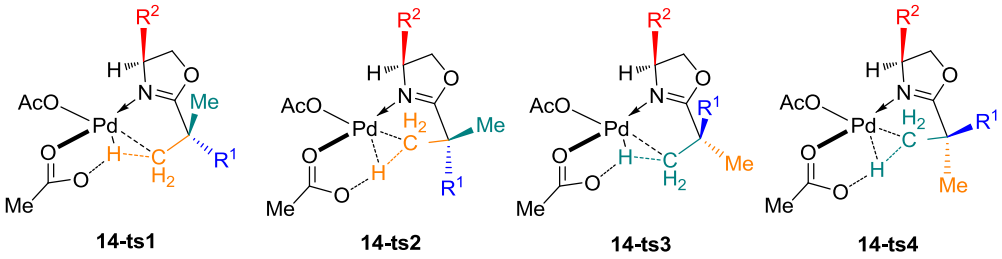

14a-ts1, **14a-ts2**, **14a-ts3**, **14a-ts4:** R^1 = *t*-Bu, R^2 = *t*-Bu
14b-ts1, **14b-ts2**, **14b-ts3**, **14b-ts4:** R^1 = Et, R^2 = *t*-Bu
14c-ts1, **14c-ts2**, **14c-ts3**, **14c-ts4:** R^1 = Et, R^2 = *i*-Pr

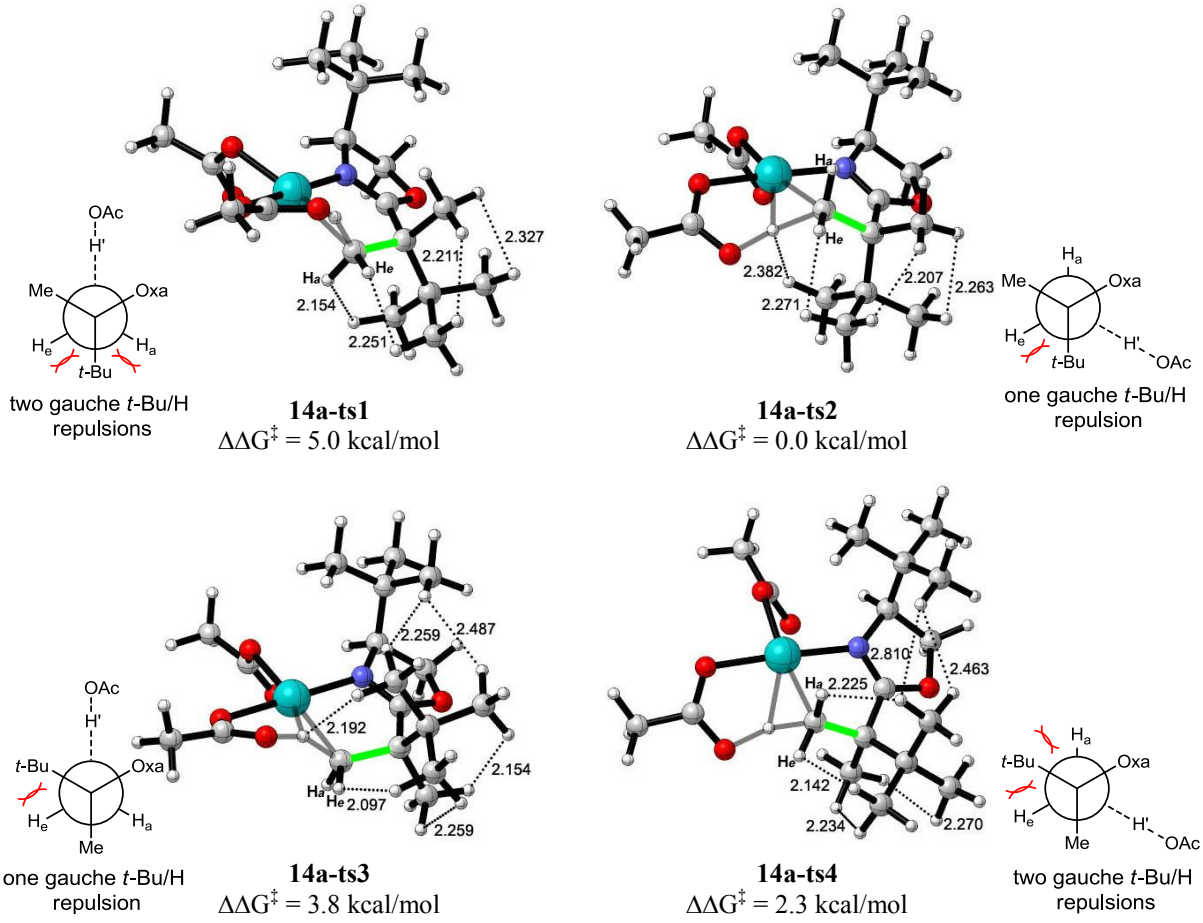

Figure 4. Optimized geometries of transition states **14a-ts1**, **14a-ts2**, **14a-ts3**, and **14a-ts4** and the Newman projections about the C–C bond highlighted in green.

Table 1. Relative activation free energies and enthalpies (in parentheses) for the C–H activation transition states. All energies are with respect to **14-ts2** in kcal/mol.

oxazoline	R^1	R^2	**14-ts1**	**14-ts2**	**14-ts3**	**14-ts4**	*de* (calc.)	*de* (exp.)
2a	*t*-Bu	*t*-Bu	5.0 (4.7)	0.0 (0.0)	3.8 (3.4)	2.3 (2.2)	96% (96%)	82%
2b	Et	*t*-Bu	2.8 (3.0)	0.0 (0.0)	3.6 (3.0)	0.1 (0.2)	8% (17%)	25%
2c	Et	*i*-Pr	0.3 (0.6)	0.0 (0.0)	0.8 (0.5)	-0.2 (-0.1)	17% (8%)	0 %

The energy difference between **14a-ts2** and **14a-ts4** is attributed to the *gauche*-*t*-Bu/H repulsions around the prochiral carbon–methyl bond (highlighted in green in Figure 4). The cleaving C–H bond is *gauche* to the adjacent *t*-Bu group in **14a-ts2** and *anti* to the *t*-Bu in **14a-ts4** (see the Newman projections in Figure 4). Because the C–H distances in the cleaving C–H bond (~1.4 Å) is significantly longer than a regular C–H bond (~1.1 Å), the *gauche t*-Bu/H repulsion with the cleaving C–H bond is smaller. In **14a-ts2**, there is one regular *gauche t*-Bu/H interaction with an H–H distance of 2.27 Å between *t*-Bu and H_e. The *gauche* repulsion with the cleaving C–H' bond is much weaker, with a significantly longer H–H distance of 2.38 Å between *t*-Bu and H'. In contrast, there are two hydrogens *gauche* to the *t*-Bu in **14a-ts4**, with H–H distances being 2.14 and 2.22 Å, respectively. Thus, **14a-ts4** is less stable than **14a-ts2** due to unfavorable *gauche t*-Bu/H repulsions. Replacing the *t*-Bu (R^1) group with smaller Et, the energy differences between transition states **14b-ts2** and **14b-ts4** and between **14c-ts2** and **14c-ts4** reduced to essentially zero, in agreement with experiment. The *gauche* repulsions between Et and H are much smaller than the *t*-Bu/H repulsions. The Et substitution on R^1 is not sufficient to differentiate the activation of *anti* and *gauche* C–H bonds as illustrated in the Newman projections in Figure 4.

3. Conclusions

We have prepared and characterized the major diastereomer of a chiral trinuclear palladacycle that exists as a potential intermediate in the oxazoline-directed, Pd(II)-catalyzed iodination and acetoxylation of sp^3 C–H bonds. Reaction of the chiral trinuclear palladacycle with I_2 provided the iodinated product in the same diastereomeric ratio as that of the catalytic reaction (dr, 91:9). The solid state structure of the major diastereomer ***syn*-(*S*,*S*)-10a** revealed that the two bulky *t*-butyl groups on the oxazoline and carboxylic moieties of the substrate remain in *anti*-positions to each other, and that the new chiral center

generated after the C–H cleavage assumed (*S*) stereochemistry. Computational investigations on reactivities and diastereoselectivities of C–H activation of oxazolines **2a-c** provided good agreement with the experimental results. In the most preferred transition state, in which the bulky *t*-Bu substituents on the prochiral carbon (R^1) and on the oxazoline (R^2) prefer to be *anti* to each other, leads to the major diastereomer product ***syn*-(*S*,*S*)-10a**. *t*-Bu substitution at the R^2 position is essential to achieve high reactivity. Replacing the R^2 group with the smaller Et group leads to formation of a stable resting [bis(oxazoline)]$Pd(OAc)_2$ complex before the C–H activation and increases the overall activation barrier. In the reaction with *t*-Bu substituted oxazoline **2a**, such [bis(oxazoline)]$Pd(OAc)_2$ complex is destabilized to form the reactive monomeric intermediate (oxazoline)$Pd(OAc)_2$ due to steric repulsions with the *t*-Bu groups.

4. Experimental

4.1. Preparation of Trinuclear Bis-*μ*-acetato and Bis-*μ*-trifluoroacetato Pd(II) Complexes 9a and 10a. Oxazoline **2a** (113 mg, 0.5 mmol) was stirred with palladium acetate (168 mg, 0.75 mmol) in CH_2Cl_2 (5 ml) at 24 °C for 48 h. The solvent was removed in a rotary evaporator to give a pale green complex **9a**. This complex is highly soluble in *n*-pentane even at −18 ºC. The crude complex **9a** was stirred in trifluoroacetic anhydride (1 mL) for 24 h at room temperature. The excess of anhydride was removed in a rotary evaporator and the residue was washed with cold *n*-pentane (0.2 mL × 2) and dried under high vacuum to afford a green complex **10a** as a mixture of two isomers in a 91:9 ratio (225 mg, 84% yield). The complex was characterized by NMR spectroscopy. ^{1}H NMR (400 MHz, CD_2Cl_2) δ 0.92 (s, 9H × 0.91), 1.02 (s, 9H), 1.05 (s, 9H × 0.09), 1.32 (s, 3H × 0.09), 1.46 (s, 3H × 0.91), 2.34 (d, J = 8.0 Hz, 1H × 0.91), 2.52 (d, J = 8.0 Hz, 1H × 0.09), 3.00 (d, J = 8.0 Hz, 1H × 0.09), 3.37 (d, J = 8.0 Hz, 1H × 0.91), 3.46 (d, J = 8.0 Hz, 1H), 4.21 (t, J = 8.0 Hz, 1H × 0.91), 4.27 (t, J = 8.0 Hz, 1H × 0.09), 4.56 (d, J = 8.0 Hz, 1H); ^{13}C NMR (100 MHz, CD_2Cl_2) δ 14.0, 21.5, 22.5, 23.8, 24.9, 25.6, 25.8, 25.9, 26.0, 26.1, 34.4, 34.5, 34.7, 35.3, 50.4, 51.1, 70.3, 70.8, 71.2, 71.3, 184.9, 185.5.

4.2. Crystallization of *syn*-(*S*,*S*)-10a. The complex **10a** was dissolved in *n*-pentane at room temperature and filtered through a Cameo 3N syringe filter (0.45 μ, 3 mm) (Osmonics Inc.) in a glass sample vial. The complex was crystallized as green prisms in 24 hours at −18 °C. The green prismatic crystals were characterized by X-ray crystallography.

4.3. Computational Methodology. Geometries were optimized with B3LYP and the SDD basis set for Pd and the 6-31G(d) basis set for other atoms. Single point energies were calculated at the M06/SDD–6-311++G(d,p) level. The reported free energies and enthalpies include zero-point energies and thermal corrections calculated at 298K with B3LYP/SDD–6-31G(d). All calculations were performed with Gaussian 09.[28]

Acknowledgement. We gratefully acknowledge TSRI and NSF Center for Stereoselective C–H Functionalization (CHE-0943980) and the National Science Foundation (CHE-1059084, KNH) for financial support of this research. Calculations were performed on the Hoffman2 cluster at UCLA and the Extreme Science and Engineering Discovery Environment (XSEDE), which is supported by the NSF.

Supporting Information Available. Experimental procedures, characterization of the complex ***syn*-(*S*,*S*)-10a**, complete ref. 28 and computational details. This material is available free of charge *via* the internet at http://pubs.acs.org.

References

1. (a) Hartwig, J. F. *Nature* **2008,** *455*, 314. (b) Hartwig, J. F.; Cook, K. S.; Hapke, M.; Incarvito, C. D.; Fan, Y. B.; Webster, C. E.; Hall, M. B. *J. Am. Chem. Soc.* **2005,** *127*, 2538. (c) Du Bois, J. *Chemtracts* **2005,** *18*, 1. (d) Periana, R. A.; Bhalla, G.; Tenn, W. J.; Young, K. J. H.; Liu, X. Y.; Mironov, O.; Jones, C. J.; Ziatdinov, V. R. *J. Mol. Catal. A* **2004,** *220*, 7. (e) Crabtree, R. H. *J. Organomet. Chem.* **2004,** *689*, 4083. (f) Stahl, S. S.; Labinger, J. A.; Bercaw, J. E. *Angew. Chem. Int. Ed.* **1998,** *37*, 2180. (g) Sen, A. *Acc. Chem. Res.* **1998,** *31*, 550. (h) Shilov, A. E.; Shul'pin, G. B. *Chem. Rev.* **1997,** *97*, 2879. (i) Ryabov, A. D. *Chem. Rev.* **1990,** *90*, 403.

2. Davies, H. M. L.; Beckwith, R. E. J., *Chem. Rev.* **2003,** *103*, 2861.

3. (a) Yu, J. Q.; Giri, R.; Chen, X. *Org. Biomol. Chem.* **2006,** *4*, 4041. (b) Daugulis, O.; Zaitsev, V. G.; Shabashov, D.; Pham, Q. N.; Lazareva, A. *Synlett* **2006**, 3382. (c) Lyons, T. W.; Sanford, M. S. *Chem. Rev.* **2010,** *110*, 1147.

4. (a) Garcia-Cuadrado, D.; de Mendoza, P.; Braga, A. A. C.; Maseras, F.; Echavarren, A. M. *J. Am. Chem. Soc.* **2007,** *129*, 6880. (b) Garcia-Cuadrado, D.; Braga, A. A. C.; Maseras, F.; Echavarren, A. M. *J. Am. Chem. Soc.* **2006,** *128*, 1066.

5. Davies, D. L.; Donald, S. M. A.; Macgregor, S. A. *J. Am. Chem. Soc.* **2005,** *127*, 13754.

6. Gorelsky, S. I.; Lapointe, D.; Fagnou, K. *J. Am. Chem. Soc.* **2008,** *130*, 10848.

7. (a) Lafrance, M.; Gorelsky, S. I.; Fagnou, K. *J. Am. Chem. Soc.* **2007,** *129*, 14570. (b) Lafrance, M.; Rowley, C. N.; Woo, T. K.; Fagnou, K. *J. Am. Chem. Soc.* **2006,** *128*, 8754. (c) Rousseaux, S.; Gorelsky, S. I.; Chung, B. K. W.; Fagnou, K. *J. Am. Chem. Soc.* **2010,** *132*, 10692. (d) Balcells, D.; Clot, E.; Eisenstein, O. *Chem. Rev.* **2010,** *110*, 749. (e) Ke, Z.; Cundari, T. R. *Organometallics* **2010,** *29*, 821. (f) Musaev, D. G.; Kaledin, A.; Shi, B. F.; Yu, J. Q. *J. Am. Chem. Soc.* **2012,** *134*, 1690.

8. (a) Gomez, M.; Granell, J.; Martinez, M. *J. Chem. Soc., Dalton Trans.* **1998**, 37. (b) Ryabov, A. D.; Sakodinskaya, I. K.; Yatsimirsky, A. K. *J. Chem. Soc., Dalton Trans.* **1985**, 2629. (c) Dick, A. R.; Kampf, J. W.; Sanford, M. S. *J. Am. Chem. Soc.* **2005,** *127*, 12790. (d) Powers, D. C.; Ritter, T. *Nature Chem.* **2009,** *1*, 302. (e) Powers, D. C.; Geibel, M. A. L.; Klein, J. E. M. N.; Ritter, T. *J. Am. Chem. Soc.* **2009,** *131*, 17050. (f) Khusnutdinova, J. R.; Rath, N. P.; Mirica, L. M. *J. Am. Chem. Soc.* **2010,** *132*, 7303.

9. (a) Giri, R.; Liang, J.; Lei, J. G.; Li, J. J.; Wang, D. H.; Chen, X.; Naggar, I. C.; Guo, C. Y.; Foxman, B. M.; Yu, J. Q. *Angew. Chem. Int. Ed.* **2005,** *44*, 7420. (b) Giri, R.; Chen, X.; Yu, J. Q. *Angew. Chem. Int. Ed.* **2005,** *44*, 2112.

10. Giri, R.; Shi, B.-F.; Engle, K. M.; Maugel, N.; Yu, J.-Q., *Chem. Soc. Rev.* **2009,** *38*, 3242.

11. (a) Whitesides, T. H.; Arhart, R. W. *Tetrahedron Lett.* **1972,** *13*, 297. (b) Schroder, D.; Schwarz, H. *J. Am. Chem. Soc.* **1993,** *115*, 8818. (c) Schroder, D.; Zummack, W.; Schwarz, H. *J. Am. Chem. Soc*. **1994,** *116*, 5857. (d) Loos, J.; Schroder, D.; Zummack, W.; Schwarz, H. *Int. J. Mass Spectrom.* **2002,** *217*, 169. (e) Hornung, G.; Schroder, D.; Schwarz, H. *J. Am. Chem. Soc.* **1997,** *119*, 2273. (f) Ma, Y. O.; Bergman, R. G. *Organometallics* **1994,** *13*, 2548. (g) Mobley, T. A.; Bergman, R. G. *J. Am. Chem. Soc.* **1998,** *120*, 3253.

12. Keyes, M. C.; Young, V. G.; Tolman, W. B. *Organometallics* **1996,** *15*, 4133.

13. Johnson, J. A.; Ning, L.; Sames, D. *J. Am. Chem. Soc.* **2002,** *124*, 6900.

14. (a) Eames, J.; Watkinson, M. *Angew. Chem. Int. Ed.* **2001,** *40*, 3567. (b) Covell, D. J.; White, M. C. *Angew. Chem. Int. Ed.* **2008,** *47*, 6448.

15. (a) Groves, J. T.; Viski, P. *J. Am. Chem. Soc.* **1989,** *111*, 8537. (b) Larrow, J. F.; Jacobsen, E. N. *J. Am. Chem. Soc.* **1994,** *116*, 12129.

16. (a) Thalji, R. K.; Ellman, J. A.; Bergman, R. G. *J. Am. Chem. Soc.* **2004,** *126*, 7192. (b) Harada, H.; Thalji, R. K.; Bergman, R. G.; Ellman, J. A. *J. Org. Chem.* **2008,** *73*, 6772.

17. (a) Zalatan, D. N.; Du Bois, J. *J. Am. Chem. Soc.* **2008,** *130*, 9220. (b) Liang, J. L.; Yuan, S. X.; Huang, J. S.; Yu, W. Y.; Che, C. M. *Angew. Chem. Int. Ed.* **2002,** *41*, 3465.

18. (a) Evans, D. A.; Bartroli, J.; Shih, T. L. *J. Am. Chem. Soc.* **1981,** *103*, 2127. (b) Meyers, A. I. *Acc. Chem. Res.* **1978,** *11*, 375. (c) Ellman, J. A.; Owens, T. D.; Tang, T. P. *Acc. Chem. Res.* **2002,** *35*, 984. (d) Myers, A. G.; Yang, B. H.; Chen, H.; McKinstry, L.; Kopecky, D. J.; Gleason, J. L. *J. Am. Chem. Soc.* **1997,** *119*, 6496.

19. Meyers, A. I. *J. Org. Chem.* **2005,** *70*, 6137.

20. Hargaden, G. C.; Guiry, P. J. *Chem. Rev.* **2009,** *109*, 2505.

21. (a) Balavoine, G.; Clinet, J. C.; Zerbib, P.; Boubekeur, K. *J. Organomet. Chem.* **1990,** *389*, 259. (b) Balavoine, G.; Clinet, J. C. *J. Organomet. Chem.* **1990,** *390*, C84.

22. A part of the current research work has been published elsewhere. Giri, R., Ph.D. Thesis, The Scripps Research Institute, 2009.

23. Moyano, A.; Rosol, M.; Moreno, R. M.; Lopez, C.; Maestro, M. A. *Angew. Chem. Int. Ed.* **2005,** *44*, 1865.

24. Giri, R.; Chen, X.; Hao, X. S.; Li, J. J.; Liang, J.; Fan, Z. P.; Yu, J. Q. *Tetrahedron-Asymmetry* **2005,** *16*, 3502.

25. *Syn*- and *anti*-geometries of the trinuclear palladacycles appear to be controlled by the steric bulk on both the oxazoline and the parent carboxylic acid moieties. However, the formation of *syn*- or *anti*-geometry is irrelevent to the observed diastereoselectivity since both geometries generate the same diastereomers.

26. Gomez, M.; Granell, J.; Martinez, M. *Organometallics* **1997,** *16*, 2539.

27. Palladium(II) acetate exists as a trimer in CH_2Cl_2 and benzene solutions. For the determination of its solution phase structures, see: (a) Stephens, T. A.; Morehous, S. M.; Powell, A. R.; Heffer, J. P.; Wilkinson, G. *J. Chem. Soc.* **1965**, 3632. (b) Bakhmutov, V. I.; Berry, J. F.; Cotton, F. A.; Ibragimov, S.; Murillo, C. A. *Dalton Trans.* **2005**, 1989.

28. Gaussian 09, Rev. B.01: Frisch, M. J.; et al., Gaussian, Inc., Wallingford CT, 2010.

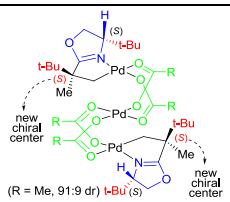

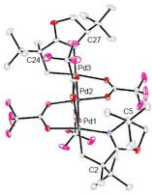

(R = CF_3, X-ray)

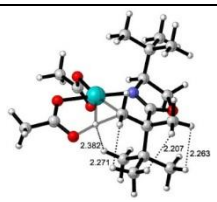

(TS for C–H activation)